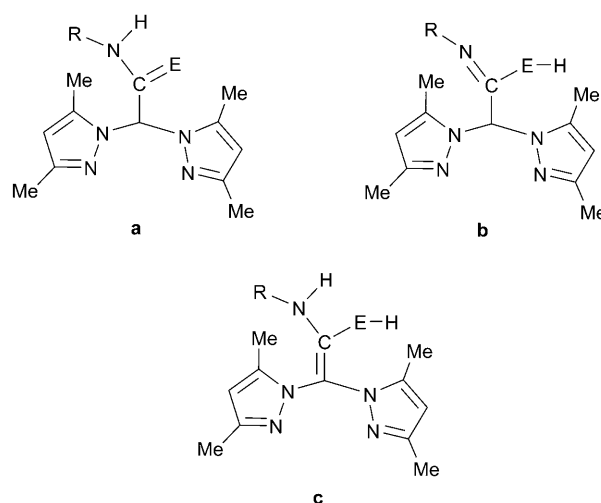


Straightforward Generation of Helical Chirality Driven by a Versatile Heteroscorpionate Ligand: Self-Assembly of a Metal Helicate by Using CH– π Interactions

Antonio Otero,^{*,[a]} Agustín Lara-Sánchez,^{*,[a]} Juan Fernández-Baeza,^[a]
 Carlos Alonso-Moreno,^[a] Juan Tejada,^[a] José A. Castro-Osma,^[a]
 Isabel Márquez-Segovia,^[a] Luis F. Sánchez-Barba,^[b] Ana M. Rodríguez,^[a] and
 M. Victoria Gómez^[a]

The assembly of architecturally sophisticated, high-nuclearity coordination complexes from the reactions of relatively simple ligands with suitable metal ions remains an area of intense activity driven not only by the aesthetic appeal of the structures, but also by the potentially wide applications of the resulting supramolecular entities as functional materials.^[1] In particular, stereochemically well-defined building blocks are needed for the assembly of metallo-supramolecular structures, the dimensions of which are greater than those found in traditional covalent-based chemistry.^[2] Helicates represent one of the paradigmatic branches of supramolecular architecture and these metallo-supramolecular arrays that contain one or more strand ligands have attracted much attention.^[3] The understanding of the interplay between the metals and the ligands in helicates and their applications in the selective preparation of complicated organised chemical architectures remains the subject of systematic investigations, with great potential applications in asymmetric synthesis^[4] and in the development of double-helical molecular architectures because life itself is encoded within double-helical DNA arrays.^[5]

Furthermore, heteroscorpionates are amongst the most versatile types of tridentate ligand and they can coordinate to a wide variety of elements.^[6,7] In the last decade our research group has contributed widely to this field, designing new heteroscorpionate ligands related to the bis(pyrazol-1-yl)methane system and incorporating several pendant donor arms.^[8] Acetamide and thioacetamide heteroscorpionate ligands exhibit high versatility in terms of coordination modes due to the existence of three possible tautomers (Scheme 1).^[9] Inspired by this versatility and taking into consideration tautomer **c**, which could be capable of forming a helical surface by attachment to metal atoms, we attempted to generate a series of single-helical dinuclear complexes that could be appropriate building blocks to self-assemble into supramolecular helical structures. Herein, we report the



Scheme 1. Tautomers of acetamide or thioacetamide heteroscorpionate ligands.

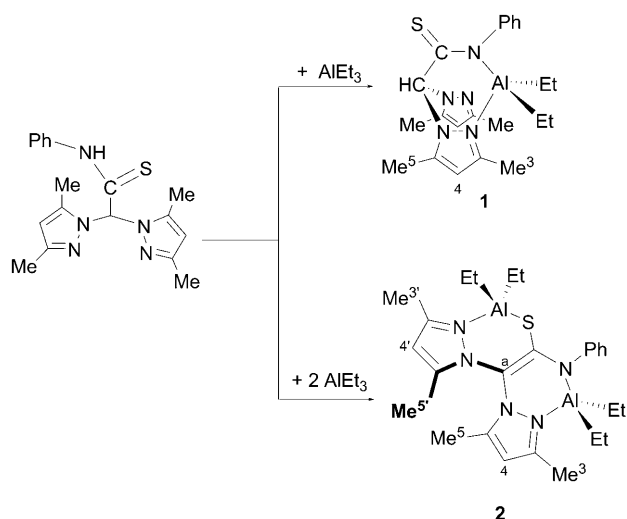
[a] Prof. Dr. A. Otero, Dr. A. Lara-Sánchez, Dr. J. Fernández-Baeza, Dr. C. Alonso-Moreno, J. Tejada, J. A. Castro-Osma, I. Márquez-Segovia, Dr. A. M. Rodríguez, Dr. M. V. Gómez
 Departamento de Química Inorgánica, Orgánica y Bioquímica
 Universidad de Castilla-La Mancha, 13071 Ciudad Real (Spain)
 Fax: (+34)926-295-318
 E-mail: antonio.otero@uclm.es
 agustin.lara@uclm.es

[b] Dr. L. F. Sánchez-Barba
 Departamento de Química Inorgánica y Analítica
 Universidad Rey Juan Carlos, 28933 Móstoles Madrid (Spain)

Supporting information for this article is available on the WWW under <http://dx.doi.org/10.1002/chem.201000694>.

synthesis of a type of binuclear organoaluminium molecular complex that presents helical chirality; this is based on the bimetallic bridging mode of the non-helical backbone heteroscorpionate ligand and a versatile and efficient self-assembly of a single-stranded helicate by using CH– π interactions.

Novel aluminium complexes containing a thioacetamidate heteroscorpionate (**1** and **2**) were synthesised (Scheme 2).



Scheme 2. Synthesis route to compounds **1** and **2**.

When the reaction was carried out with a 1:1 molar ratio of metal/ligand, the monomeric complex **1** was obtained with elimination of the corresponding ethane. However, the heteroscorpionate ligand reacted with two equivalents of AlEt_3 to yield dinuclear complex **2** by double deprotonation in a quantitative yield (95%). In this dinuclear complex the heteroscorpionate ligand is bridging two aluminium centres. The steric demands of the fixed pyrazole rings give rise to a helical surface to afford overall helical chirality. There are few cases of aluminium complexes containing ligands that are wrapped around the metal much like in a helicate.^[10]

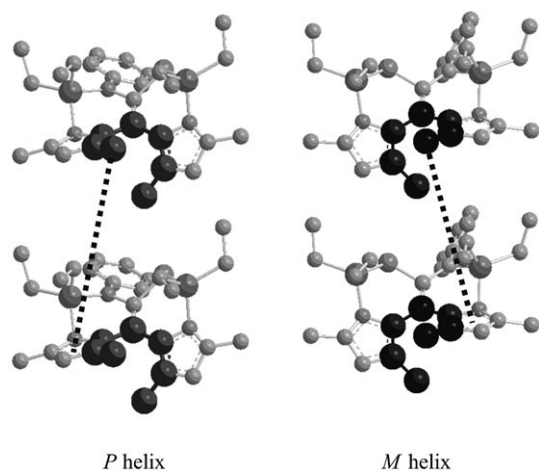


Figure 1. Schematic illustration of the helical surface in complex **2**.

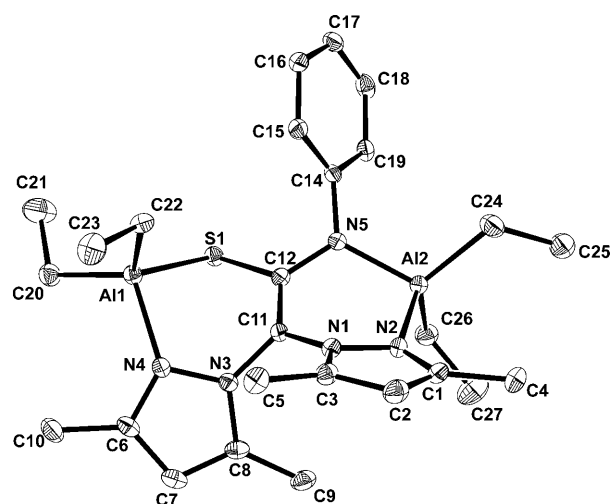


Figure 2. ORTEP view of **2** with 30% probability ellipsoids.^[14]

The helical surface for complex **2** (Figure 1) was characterised in the solid state by X-ray crystallography (discussed below). The molecular structure of complex **2** (Figure 2) exhibits a dimeric-like arrangement that is achieved through a bridging dianionic thioacetamidate fragment. The complexes adopt a bimetallic monohelical structure with each aluminium atom in a distorted tetrahedral geometry. The crystals contained two enantiomers (*M*, *P*) in the unit cell. The pyrazole rings are located in different planes. The twist angle between the two pyrazoles is $68.33(8)^\circ$.

Interestingly, the crystal structure of **2** reveals that their molecules are appropriate building blocks for the construction of a single helix by CH– π interactions, through their methyl groups of pyrazole rings.

In fact, self-assembly of the single helix in **2** gives rise to single-stranded helicates (*M* and *P*) formed along the *b* axis by CH– π interactions between a Me group (C4–H4B) of one pyrazole ring and the pyrazole ring of the other molecule (see Figures 3 and 4). The H4B–(centroid of pyrazole) distance has a value of 2.630 Å. The degree of displacement of H4B from the centre of the pyrazole ring (D_{offset}) is 0.28 Å. Although several examples of CH– π bonds as a supramolecular control element have been previously described,^[11] our helicoidal architecture constitutes a rare example in which this type of interaction is responsible for an assembly process to give an unexpected helical superstructure.^[10,12] Additionally, we observed the assembly of different chains through another intermolecular CH– π interaction established between the C10–H10B methyl of pyrazole ring and the phenyl (C14–C19) ring. The H10B–(centroid of phenyl) distance has a value of 3.325 Å and the degree of displacement of H10B from the centre of phenyl ring (D_{offset}) is 1.89 Å. These interactions give rise to a sheet extended to the *c* axis (Figure 3).

The room-temperature ^1H and $^{13}\text{C}\{^1\text{H}\}$ NMR spectra of **1** indicate the existence of a highly symmetric structure. Moreover, the broadness of some ^1H NMR signals of the heteroscorpionate ligand and ethyl groups suggest that a fluxional

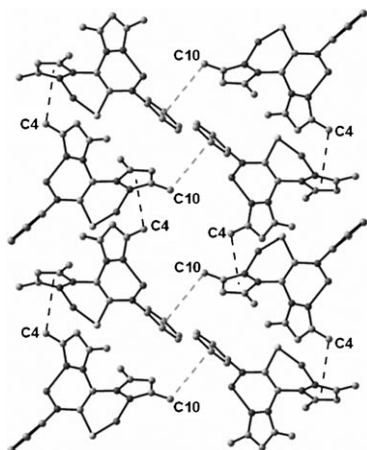


Figure 3. Ball-and-stick view (down the *a* axis) of the intermolecular interactions in complex **2**. The CH- π interactions that give rise to single-stranded helicates are marked as black dashed lines and the CH- π interactions that give rise to a sheet are marked as grey dashed lines. The hydrogen atoms and the ethyl groups of aluminium atoms are omitted for clarity.

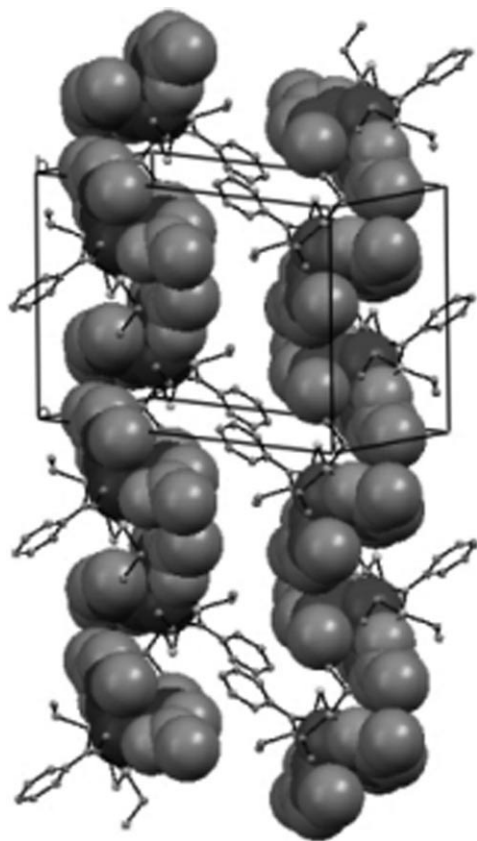


Figure 4. Space-filling view of the two adjacent *M* (left) and *P* (right) helicates for **2**.

process exists between the pyrazole rings. Variable-temperature NMR spectroscopic analysis confirms this dynamic behaviour in solution (see Figure S1 in the Supporting Information). The molecular structure of **1** was determined by X-ray analysis (see Figure S2 in the Supporting Information).

The ^1H and $^{13}\text{C}\{^1\text{H}\}$ NMR spectra of complex **2** show two singlets for each of the H^4 , Me^3 and Me^5 pyrazole protons, indicating that the two pyrazole rings are inequivalent. Four sets of signals are observed for the ethyl groups.

The NOESY 1D NMR experiments enabled the unequivocal assignment of all ^1H NMR spectroscopy resonances. These results are consistent with the above-mentioned structure for complex **2** with the heteroscorpionate ligand being wrapped around the two metal centres, coordinating through an unprecedented bimetallic bridging mode, and forming a binuclear helical aluminium compound (Scheme 2).

Concentration-dependent ^1H NMR spectroscopy measurements in $[\text{D}_6]$ benzene were performed on complex **2** in the concentration range of 50–500 mM. These measurements show a downfield shift of H^4 pyrazole protons at higher concentrations (Figure 5) accompanied by line broadening

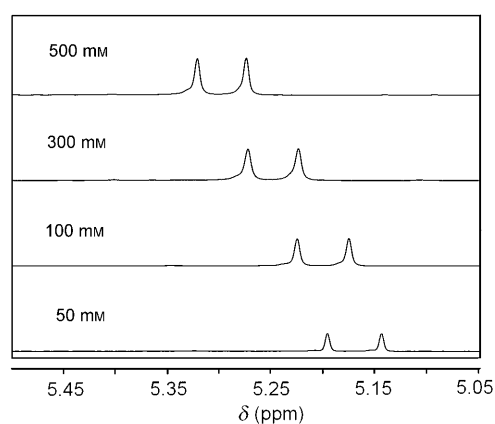


Figure 5. Concentration-dependent ^1H NMR spectra of complex **2** in C_6D_6 at 25 °C.

especially for the highest concentrations measured. These experiments indicate that there is an interaction involving the pyrazole rings, therefore, suggesting the existence of CH- π interactions in solution that would result in molecular aggregation.

Concentration-dependent ^1H pulsed field-gradient spin-echo (PFGSE) NMR spectroscopy experiments were carried out on the same samples with the aim of gaining a better insight into the behaviour of complex **2** in solution, and to further prove the tendency of aggregation of the single molecules.^[13] The translational self-diffusion coefficients (D_t) can be accurately evaluated by PFGSE NMR spectroscopy experiments, providing, in itself, important information about the strength of the CH- π interactions. PFGSE NMR spectroscopy experiments were carried out for complex **2** in $[\text{D}_6]$ benzene at 25 °C using TMS as an internal standard. The pseudo-2D DOSY spectrum of complex **2** showed a single diffusion coefficient of $(6.14 \pm 0.02) \times 10^{-10} \text{ m}^2 \text{ s}^{-1}$ (Figure 6), lower than that of the ligand ($D_t = (8.04 \pm 0.02) \times 10^{-10} \text{ m}^2 \text{ s}^{-1}$) at the same concentration (100 mM), indicating an increase in the molecular size determined by metal complexation.

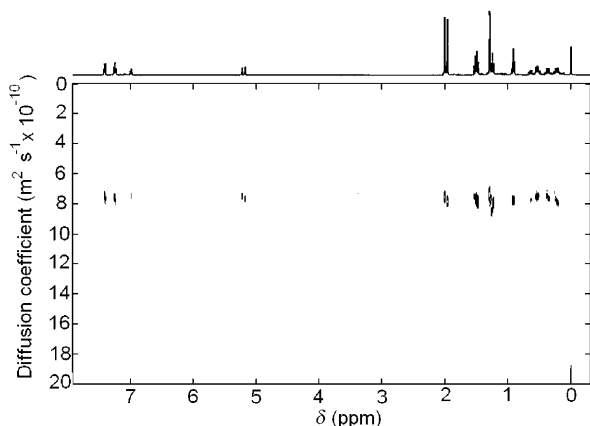


Figure 6. Pseudo-2D DOSY spectrum (500 MHz, C₆D₆, 25 °C) of complex **2** at 100 mm.

Importantly, progressive concentration experiments from 50 mm to –500 mm of complex **2** led to a roughly twofold concomitant decrease in the diffusion coefficient (Table 1), providing evidence for the self-assembly of the single molecular species of complex **2** in solution. This behaviour is in agreement with the self-assembly phenomenon observed in solid state, which led to the formation of a helicate through intermolecular CH–π interactions.

Table 1. Diffusion coefficients ($10^{-10} D_t$, m²s⁻¹) and concentrations (*C*, mm) for complex **2** in C₆D₆ at 25 °C.

<i>C</i> [mm]	<i>D_t</i> [m ² s ⁻¹]
50	7.71 ± 0.02
100	7.40 ± 0.02
300	6.14 ± 0.02
500	4.60 ± 0.02

In conclusion, we have developed a novel and straightforward approach to prepare a single-helical, dinuclear aluminium complex able to act as a building block for a single-stranded aluminium helicate self-assembled by CH–π interactions. This has been characterised by an X-ray diffraction study. Additionally, concentration-dependent ¹H and PFGSE NMR spectroscopy experiments led us to be witness of the existence of the CH–π interactions and therefore to corroborate the tendency of the single-helical species to self-assemble also in solution. Due to the fact that the nature of these types of single-helical systems have great promise as building blocks for metal–organic coordination networks, we are actively working in this interesting research field.

Experimental Section

[AlEt₂(pbptam)] (1): In a 100 mL Schlenk tube, *N*-phenyl-2,2-bis(3,5-dimethylpyrazol-1-yl)thioacetamide (pbptamH; 0.85 g, 2.50 mmol) was dissolved in dry toluene (30 mL) and cooled at 0 °C. A solution of AlEt₃

(1 M in hexane) (2.50 mL, 2.50 mmol) was added and the mixture was allowed to warm to room temperature with stirring for 1 h. The solution was concentrated and recrystallised (toluene) at –26 °C to give compound **1** as white crystals (0.95 g, 90%). ¹H NMR (500 MHz, C₆D₆, 25 °C): δ = 7.43 (s, 1H; CH), 5.34 (s, 2H; H⁴), 2.09 (s, 6H; Me³), 1.91 (s, 6H; Me³), 7.44 (d, ³*J*(H,H) = 7.2 Hz, 2H; *H_o*-PhNCS), 7.22 (t, ³*J*(H,H) = 6.9 Hz, 2H; *H_m*-PhNCS), 7.04 (t, ³*J*(H,H) = 6.8 Hz, 1H; *H_p*-PhNCS), 1.23 (t, ³*J*(H,H) = 8.0 Hz, 6H; AlCH₂CH₃), 1.50 ppm (m, 4H; AlCH₂CH₃); ¹³C[¹H] NMR (125 MHz, C₆D₆, 25 °C): δ = 75.8 (CH), 150.5, 142.5 (C^{3/5}), 107.5 (C⁴), 13.0 (Me³), 11.0 (Me³), 147.0–126.4 (*Ph*NCS), 195.1 (PhNCS), 9.5 (AlCH₂CH₃), 0.95 ppm (AlCH₂CH₃); elemental analysis calcd (%) for C₂₂H₃₀AlN₅S: C 62.39, H 7.14, N 16.53; found: C 61.98, H 7.34, N 16.31.

[Al₂Et₄(μ-pbptam)] (2): In a 100 mL Schlenk tube, pbptamH (0.85 g, 2.50 mmol) was dissolved in dry toluene (30 mL) and cooled at 0 °C. A solution of AlEt₃ (1 M in hexane) (5.00 mL, 5.00 mmol) was added and the mixture was allowed to warm to room temperature with stirring for 1 h. The solution was concentrated and recrystallised (hexane) at –26 °C to give compound **2** as white crystals (2.25 g, 95%). ¹H NMR (500 MHz, C₆D₆, 25 °C): δ = 5.21 (s, 1H; H⁴), 5.16 (s, 1H; H⁴), 2.01 (s, 3H; Me³), 1.96 (s, 3H; Me³), 1.29 (s, 6H; Me^{3,5}), 7.42 (d, ³*J*(H,H) = 8.4 Hz, 2H; *H_o*-PhNCS), 7.27 (t, ³*J*(H,H) = 6.6 Hz, 2H; *H_m*-PhNCS), 7.01 (t, ³*J*(H,H) = 6.6 Hz, 1H; *H_p*-PhNCS), 1.53, 1.51, 1.26, 0.94 (m, 12H; AlCH₂CH₃), 0.58–0.20 ppm (m, 8H; AlCH₂CH₃); ¹³C[¹H] NMR (125 MHz, C₆D₆, 25 °C): δ = 104.3 (C⁶), 149.8, 149.0, 146.1, 141.8 (C^{3,3'} or ^{5,5'}), 107.6, 107.5 (C^{4,4'}), 12.7 (Me³), 12.4 (Me³), 9.6, 9.5 (Me^{3,5}), 148.9–123.7 (*Ph*NCS), 156.7 (PhNCS), 10.0, 9.9, 9.8, 8.6 (AlCH₂CH₃), 0.6, 0.5, 0.1, –0.6 ppm (AlCH₂CH₃); elemental analysis calcd (%) for C₂₆H₃₉Al₂N₅S: C 61.51, H 7.74, N 13.80; found: C 61.92, H 8.01, N 13.45.

Acknowledgements

We gratefully acknowledge financial support from the Ministerio de Educación y Ciencia, Spain (MEC, grant nos. CTQ2008-00318/BQU and Consolider-Ingenio 2010 ORFEO CSD2007-00006) and the Junta de Comunidades de Castilla-La Mancha (grant no. PCI08-0010). M.V.G. acknowledges MICINN and Marie Curie Reintegration Grants. Mathias Nilsson is acknowledged for useful discussions on the DOSY experiments.

Keywords: aluminum • CH–π interactions • chirality • heteroscorpionate ligands • self-assembly

- [1] M. P. Suh, Y. E. Cheon, E. Y. Lee, *Coord. Chem. Rev.* **2008**, 252, 1007–1026.
- [2] a) J.-M. Lehn, *Supramolecular Chemistry-Concepts and Perspectives*, VCH, Weinheim, **1995**; b) E. C. Constable, *Prog. Inorg. Chem.* **1994**, 42, 67–138; c) *Comprehensive Supramolecular Chemistry* (Eds.: J. L. Atwood, J. E. D. Davies, J.-M. Lehn, D. D. MacNicol, F. Vögtle), Pergamon, Oxford, **1996**; d) D. Philp, J. F. Stoddart, *Angew. Chem.* **1996**, 108, 1242–1286; *Angew. Chem. Int. Ed. Engl.* **1996**, 35, 1154–1196; e) A. F. Williams, *Pure Appl. Chem.* **1996**, 68, 1285–1289.
- [3] a) M. Albrecht, *Chem. Rev.* **2001**, 101, 3457–3497; b) C. Piguet, G. Bernardinelli, G. Hopfgartner, *Chem. Rev.* **1997**, 97, 2005–2062; c) J. Childs, M. J. Hannon, *Supramol. Chem.* **2004**, 16, 2–22.
- [4] a) H.-L. Kwong, H.-L. Yeung, W.-S. Lee, W.-T. Wong, *Chem. Commun.* **2006**, 4841–4843; b) N. Takenaka, R. S. Sarangthem, B. Captain, *Angew. Chem.* **2008**, 120, 9854–9856; *Angew. Chem. Int. Ed.* **2008**, 47, 9708–9710.
- [5] For example, see: a) M. J. Hannon, L. J. Childs, *Supramol. Chem.* **2004**, 1, 7–22; b) M. J. Hannon, C. L. Painting, N. W. Alcock, *Chem. Commun.* **1999**, 2023–2024; c) J. Hamblin, F. Tuna, S. Bunce, L. J. Childs, A. Jackson, W. Errington, N. W. Alcock, H. Nierengarten, A.

- van Dorsselaer, E. Leize-Wagner, M. J. Hannon, *Chem. Eur. J.* **2007**, *13*, 9286–9296.
- [6] For example, see: a) S. Trofimenko, *Chem. Rev.* **1993**, *93*, 943–980; b) S. Trofimenko, *Prog. Inorg. Chem.* **1986**, *34*, 115–210; c) C. Pettinari, R. Pettinari, *Coord. Chem. Rev.* **2005**, *249*, 525–543; d) H. R. Bigmore, S. C. Lawrence, P. Mountford, C. S. Tredget, *Dalton Trans.* **2005**, 635–651.
- [7] For example, see: a) D. Adhikari, G. Zhao, F. Basuli, J. Tomaszewski, J. C. Huffman, D. J. Mindiola, *Inorg. Chem.* **2006**, *45*, 1604–1610; b) S. Milione, F. Grisi, R. Centore, A. Tuzi, *Organometallics* **2006**, *25*, 266–274; c) M. H. Schofield, M. L. Barros, M. G. Cushion, A. D. Scharwarz, P. Mountford, *Dalton Trans.* **2009**, 85–96.
- [8] a) A. Otero, J. Fernández-Baeza, A. Antiñolo, J. Tejada, A. Lara-Sánchez, *Dalton Trans.* **2004**, 1499–1510; b) A. Otero, J. Fernández-Baeza, A. Lara-Sánchez, J. Tejada, L. F. Sánchez-Barba, *Eur. J. Inorg. Chem.* **2008**, 5309–5326.
- [9] a) A. Otero, A. Lara-Sánchez, J. Fernández-Baeza, E. Martínez-Caballero, I. Márquez-Segovia, C. Alonso-Moreno, L. F. Sánchez-Barba, A. M. Rodríguez, *Dalton Trans.* **2010**, *39*, 930–940; b) A. Otero, J. Fernández-Baeza, A. Lara-Sánchez, C. Alonso-Moreno, I. Márquez-Segovia, L. F. Sánchez-Barba, A. M. Rodríguez, *Angew. Chem.* **2009**, *121*, 2210–2213; *Angew. Chem. Int. Ed.* **2009**, *48*, 2176–2179.
- [10] a) A. Johansson, M. Håkansson, *Chem. Eur. J.* **2005**, *11*, 5238–5248; b) T. Kaczorowski, I. Justyniak, T. Lipińska, J. Lipkowski, J. Lewiński, *J. Am. Chem. Soc.* **2009**, *131*, 5393–5395.
- [11] For example, see: a) L. J. Childs, M. Pasco, A. J. Clarke, N. W. Alcock, M. J. Hannon, *Chem. Eur. J.* **2004**, *10*, 4291–4300; b) K. N. Houk, S. Menzer, S. P. Newton, F. M. Raymo, J. F. Stoddard, D. J. Williams, *J. Am. Chem. Soc.* **1999**, *121*, 1479–1487; c) V. R. Thalladi, H. C. Weiss, D. Blaser, R. Boese, A. Nangia, G. R. Desiraju, *J. Am. Chem. Soc.* **1998**, *120*, 8702–8710.
- [12] Only a few examples of helicates in which the ligand strand is built up by using hydrogen bonding has been previously described: a) S. G. Telfer, T. Sato, R. Kuroda, *Angew. Chem.* **2004**, *116*, 591–594; *Angew. Chem. Int. Ed.* **2004**, *43*, 581–584; b) S. G. Telfer, R. Kuroda, *Chem. Eur. J.* **2005**, *11*, 57–68.
- [13] A. Macchioni, G. Ciancaleoni, C. Zuccaccia, D. Zuccaccia, *Chem. Soc. Rev.* **2008**, *37*, 479–489.
- [14] CCDC-756898 contains the supplementary crystallographic data for this paper. These data can be obtained free of charge from The Cambridge Crystallographic Data Centre via www.ccdc.cam.ac.uk/data_request/cif.

Received: March 18, 2010
Published online: June 25, 2010